



Natural product inspired allicin analogs as novel anti-cancer agents

Ishani Bhaumik^{a,1}, Kunal Pal^{a,1}, Utsab Debnath^a, Parimal Karmakar^b, Kuladip Jana^a, Anup Kumar Misra^{a,*}

^a Bose Institute, Division of Molecular Medicine, P-1/12, C.I.T. Scheme VII M, Kolkata 700054, India

^b Department of Life Science and Biotechnology, Jadavpur University, Kolkata 700 032, India

ARTICLE INFO

Keywords:

Sulphenyl sulfoxide
Allicin, garlic
Anti-cancer
ROS
Caspase 3
Apoptosis

ABSTRACT

A series of novel analogs of Allicin (S-allyl prop-2-ene-1-sulfinothioate) present in garlic has been synthesized in high yield. Synthesized 23 compounds were evaluated against different breast cancer cells (MDA-MB-468 and MCF-7) and non-cancer cells (WI38). Four compounds (**3f**, **3h**, **3m** and **3u**) showed significant cytotoxicity against cancer cells whereas nontoxic to the normal cells. Based on the LD₅₀ values and selectivity index (SI), compound **3h** (S-p-methoxybenzyl (p-methoxyphenyl)methanesulfinothioate) was considered as most promising anticancer agent amongst the above three compounds. Further bio-chemical studies confirmed that compound **3h** promotes ROS generation, changes in mitochondrial permeability transition and induced caspase mediated DNA damage and apoptosis.

1. Introduction

In spite of enormous technological and social development, cancer is still one of the most common diseases of concern and a leading cause of human suffering and death [1,2]. The alarming rise in incidence of new types of cancer and the public burden represents a crisis for public health and health systems worldwide [3]. Detailed analyses of pathways and mechanisms for the spreading of cancer and identification of several antitumor agents have led to significant developments in the prevention and treatment of cancer [4,5]. Chemotherapy, irradiation and immunotherapy are the gold standard approaches for the treatment of cancer worldwide in spite of their toxicity. In the second line, use of natural products from plants and animals and their derivatives have produced remarkable leads for the treatment of cancer [6–10]. Due to the toxicity of currently used therapeutics for the treatment of various types of tumors, several natural products and their structural derivatives have been evaluated for their potential to act as anti-cancer agents [11,12]. A wide range of natural products e.g. terpenoids [13,14], flavonoids [15], alkaloids [16], polyesters, polyphenols [17] and other secondary metabolites have shown promising anticancer properties. Several attempts were made to functionalize the naturally occurring molecules or preparation of their analogs using modern synthetic strategies for the development of potential chemotherapeutic agents from the natural products against cancer with higher efficacy and lower toxicity [18–21]. Hence the current thrust is to develop alternate

strategies of therapeutics, primarily through the chemical modifications of compounds isolated from natural sources or by conjugating some compounds with an appropriate pharmacophore to increase efficacy and minimize toxicity.

Garlic (*Allium sativum*) contains several organosulfur compounds, which protects it from the attack of bacteria, fungi and animals [22]. Alliin is one of the natural constituents of garlic, which is a sulfoxide containing amino acid [23]. During the process of chopping or crushing of fresh garlic, alliin is converted into allicin (allylsulphenyl allylsulfoxide or S-allyl prop-2-ene-1-sulfinothioate) by the action of alliinase enzyme, which is responsible for the aroma of garlic [24]. Recently, garlic (*Allium sativum*) extracts and garlic-derived compounds have received increasing attention due to their antiproliferative activities against different types of cancer cells [25,26]. Allicin is a thioester of sulfenic acid, which is relatively unstable and changes into disulfide derivatives such as diallyl disulfide [27]. It appears as a colorless oil with distinctive malodorous smell. Although Allicin is a chiral compound it occurs naturally as a racemate [28]. In the past, Allicin has been shown to possess several medicinal potential such as anticancer, antioxidant and antimicrobial properties by inducing apoptosis, regulation of cell cycle progression and signal transduction [29–31]. Taking clue from the biological activities of allicin, it is pertinent to synthesize novel analogs of allicin using a generalized reaction condition to evaluate their pharmaceutical potential as anti-cancer agents. Therefore, efficient synthesis and biological evaluation of a series of allicin analogs are

* Corresponding author.

E-mail address: anup@jcbose.ac.in (A.K. Misra).

¹ Contributed equally.



Scheme 1. Preparation of alkyl and aryl disulfide derivatives [37,38].

presented herein. In addition to the sulfide sulfoxide analogs of allicin, a series of selenium substituted analogs were also prepared with an expectation of getting better biological response. In the recent past several selenium containing natural product analogs showed highly promising anti-cancer potential [32–36]. Furthermore, several biochemical and microscopic experiments have been carried out to establish the anti-cancer potential of the most promising compound as well as its mode of action.

2. Results and discussion

2.1. Chemistry

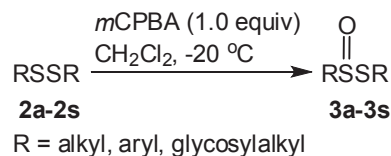
2.1.1. Synthesis of alkyl/arylsulfinyl alkyl/arylsulfoxide derivative

The target compounds were prepared using a two step reaction sequence. A series of alkyl and aryl disulfide derivatives were prepared in high yield following the reaction conditions reported earlier [37] (Scheme 1). Treatment of a series of alkyl halides with an equimolar combination of $\text{Na}_2\text{S} \cdot 9\text{H}_2\text{O}$ and CS_2 in DMF at room temperature resulted in the formation of dialkyl disulfides in high yield. In another experiment, treatment of aryl thiols with 65% nitric acid in CH_2Cl_2 at room temperature [38] led to the formation of diaryl disulfides in satisfactory yield (Scheme 1).

Having the disulfides at hand, efforts have been given for the controlled oxidation of disulfide bond to achieve a single sulfoxide moiety in the molecules. In a set of initial experiments, dibenzyl disulfide (**1g**) was treated with a variety of oxidizing agents [such as H_2O_2 , KMnO_4 , *m*-chloroperbenzoic acid (*m*CPBA), sodium periodate (NaIO_4) etc.] in different stoichiometric quantity in commonly used organic solvents (Table 1). After a series of experimentation it was observed that use of 1.0 equiv. of *m*CPBA in dichloromethane could furnish the desired product efficiently without formation of by products in 1 h at -20°C .

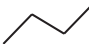
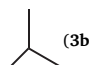
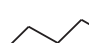
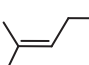
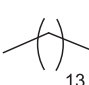
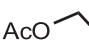
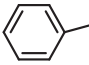
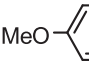
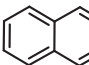
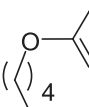
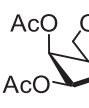
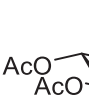

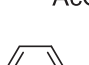
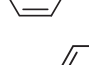
Table 1
Optimization for the preparation of benzylsulfinyl benzylsulfoxide.

Sl. No.	$ \begin{array}{ccc} \text{BnSSBn} & \xrightarrow[\text{Solvent, } -20^\circ\text{C} - \text{RT}]{\text{Oxidising agent}} & \text{BnSS(=O)Bn} \\ \text{(1g)} & & \text{(2g)} \end{array} $				
	Oxidizing agent	Equiv.	Solvent	Time (h)	Yield (%)
1	<i>m</i> CPBA	1.0	CH_2Cl_2	1	74
2	<i>m</i> CPBA	0.5	CH_2Cl_2	2	46
3	<i>m</i> CPBA	0.5	CH_2Cl_2	4	45
4	<i>m</i> CPBA	0.2	CH_2Cl_2	3	20
5	<i>m</i> CPBA	1.0	Toluene	3	10
6	<i>m</i> CPBA	1.0	Toluene	7	25
7	<i>m</i> CPBA	1.0	THF	3	8
8	<i>m</i> CPBA	1.0	CH_3OH	4	–
9	H_2O_2	1.0	CH_2Cl_2	4	–
10	KMnO_4	1.0	CH_2Cl_2	4	–
11	NaIO_4	1.0	CH_2Cl_2	4	–



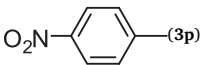
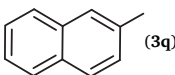
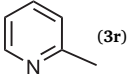
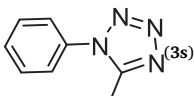
Scheme 2. Preparation of alkyl/arylsulfinyl alkyl/arylsulfoxide derivatives.

Table 2
Preparation of alkyl/arylsulfinyl alkyl/arylsulfoxide derivatives.

Sl. No.	RSSR (2) → RS(O)SR (3) R:	Time (h)	Yield (%)	Refs.
1	 (3a)	1.0	72	37,38
2	 (3b)	1.0	70	41
3	 (3c)	1.0	74	42
4	 (3d)	1.0	69	43
5	 (3e)	1.0	72	44
6	 (3f)	1.0	68	–
7	 (3g)	1.0	74	45
8	 (3h)	1.0	73	–
9	 (3i)	2.0	66	–
10	 (3j)	1.5	68	–
11	 (3k)	1.5	65	–
12	 (3l)	1.5	64	–
13	 (3m)	1.5	68	–
14	 (3n)	1.0	72	46
15	 (3o)	1.0	70	47

(continued on next page)

Table 2 (continued)

Sl. No.	RSSR (2) → RS(O)SR (3) R:	Time (h)	Yield (%)	Refs.
16	 (3p)	1.0	78	–
17	 (3q)	1.0	75	–
18	 (3r)	1.5	73	⁴⁸
19	 (3s)	1.5	71	–

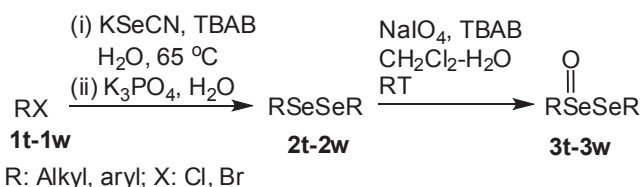
Dichloromethane was found to be superior among several organic solvents used in this reaction. Following the optimized reaction condition, a series of alkyl/arylsulfonyl alkyl/arylsulfoxide derivatives (**3a–3s**) were prepared and characterized by spectroscopic analysis (Scheme 2, Table 2).

After achieving the sulfonylsulfoxide derivatives, attention was given towards the preparation of their selenium analogs. For this purpose, alkyl diselenides were prepared from the alkyl halides following a recently developed aqueous medium reaction condition [39]. Treatment of alkyl halides with potassium selenocyanate (KSeCN) in water followed by alkaline hydrolysis resulted in the formation of dialkyl diselenides in satisfactory yield. Following optimized reaction condition in the case of disulfides (Table 1), diselenide derivatives were treated with equimolar quantity of *m*CPBA in CH₂Cl₂ at low temperature to ambient temperature. Surprisingly no required oxidized product was obtained and the diselenide remained unaffected. After screening a series of other oxidants [e.g. H₂O₂, KMnO₄ and sodium periodate (NaIO₄)] satisfactory yield of the selenenyl selenoxide derivative was obtained in satisfactory yield by the treatment with NaIO₄ (1.0 equiv.) in a phase transfer reaction condition using CH₂Cl₂ and water (5:1) in the presence of tetrabutylammonium bromide (TBAB) at room temperature [40]. Following the optimized reaction condition a series of selenenyl selenoxide derivatives were prepared in good yield and characterized using spectroscopic analysis (Scheme 3, Table 3).

2.2. Biology

2.2.1. Selective cytotoxicity of synthesized compounds towards the cancer cells

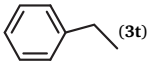
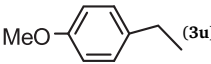
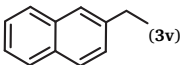
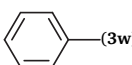
The synthesized allicin analogs (**3a–w**) along with etoposide were assessed for their ability to block proliferation of MDA-MB-468 [human triple negative (ER-, PR- and HER2-) breast cancer cells], MCF-7 [human (ER+, PR+ and HER2-) breast cancer cells] and WI-38 cells (lung fibroblast cells). The above mentioned breast cancer cells are extensively used for the screening of potential anti-breast cancer agents.



Scheme 3. Preparation of alkyl/aryl diselenide derivatives and their selective oxidation.

Table 3

Preparation of alkyl/arylselenenyl alkyl/arylselenoxide derivatives.

Sl. No.	RSeSeR (2) → RSe(O)SeR (3) R:	Time (h)	Yield (%)	Refs.
1	 (3t)	1.0	74	–
2	 (3u)	1.0	74	–
3	 (3v)	1.0	73	–
4	 (3w)	1.0	74	⁴⁹

For this experiment, cells were treated with varied concentrations of the compounds (0–50 μM) and cell proliferation was measured by MTT assay [50,51]. The anti-proliferative activities of the tested compounds in terms of LD₅₀ were presented in Table 4. From the MTT assay it was observed that four compounds (**3f**, **3h**, **3m** and **3u**) showed significantly higher efficacy in inhibiting the proliferation of MDA-MB-468 cells with LD₅₀ values of 18.87 ± 1.89 μM, 11.34 ± 2.11 μM, 22.38 ± 4.22 μM and 14.11 ± 4.13 μM respectively. Similar efficacy of **3f**, **3h**, **3m** and **3u** was observed in MCF-7 cells with LD₅₀ value of 22.36 ± 2.11 μM, 13.01 ± 2.98 μM, 25.92 ± 3.11 μM and 26.28 ± 5.87 μM and for MCF-7 cells respectively. Subsequently, when the selectivity index (SI) compounds were calculated by comparing the cytotoxic LD₅₀ value of the compounds in normal cell (WI-38) versus cancer cells (MDA-MB-468 and MCF-7) and it was observed that compound **3h** possessed highest SI (SI = 4.59 ± 0.71 and 4.00 ± 0.54) as compared to compound **3m** (SI = 3.56 ± 0.69 and 3.08 ± 0.24), compound **3f** (SI = 2.90 ± 0.14 and 2.45 ± 0.08) and compound **3u** (SI = 3.68 ± 1.12 and 1.97 ± 0.23). Etoposide, a prevalent chemotherapeutic drug for breast cancer therapy has been considered as positive control [52]. Based on the preliminary data, compound **3h** was considered as a potent anti-cancer agent on the basis of its highest selectivity index (Fig. 1).

In order to study the mechanism of action of the cytotoxicity against the cancer cells of the most promising compound **3h** based on the selectivity index (SI = 4.59 ± 0.71 in MDA-MB-468 and 4.00 ± 0.54 in MCF-7), the induction of apoptosis was measured using Annexin V-FITC/PI staining [53]. After treatment of MDA-MB-468 and MCF-7 cells with different concentrations of compound **3h** (0, 5, 10 and 15 μM) for 24 h, the flow cytometry analysis showed significant induction of apoptosis in a concentration dependent manner in the cancer cells in comparison with the non-cancer cells (WI38). Quite evidently, compound **3h** was able to induce more than 60% apoptosis in MDA-MB-468 and 58% in MCF-7 cells at 15 μM dose as shown in Fig. 2. From the AnnexinV-FITC/PI staining on the cancer cells (MDA-MB-468 and MCF-7) and non-cancer cell lines (WI38), it was observed that there is no substantial apoptosis in case of the non-cancer cells treated with compound **3h** while in case of the cancer cells the percentage of apoptotic cell is quite high. Therefore, it was decided to identify the mechanism of the induction of apoptosis in cancer cells by compound **3h** using a series of biochemical and microscopic analysis.

2.2.2. Treatment of compound 3h promotes ROS generation, mitochondrial permeability transition (MPT) in cancer cells.

Generation of reactive species (ROS) [54] is a critical phenomenon linked with several antiproliferative processes. Therefore, ROS production in response to the treatment with compound **3h** was measured by 2',7'-dichlorofluorescein diacetate (DCFDA) staining method [55].

Table 4

The LD₅₀ (μM) values of the compounds **3a-w** for the inhibition of proliferation of cancer cell lines.

Sl. No.	Compound	MDA-MB-468	MCF-7	WI38	Selectivity index (SI) in MDA-MB-468	Selectivity index (SI) in MCF-7
1	3a	26.43 ± 2.65	39.85 ± 3.65	56.77 ± 5.77	2.14 ± 0.004	1.42 ± 0.017
2	3b	52.13 ± 3.98	33.21 ± 4.49	64.32 ± 7.65	1.23 ± 0.053	1.93 ± 0.02
3	3c	66.78 ± 2.98	64.58 ± 3.76	87.66 ± 3.19	1.31 ± 0.013	1.35 ± 0.02
4	3d	29.78 ± 3.11	40.68 ± 4.98	23.89 ± 5.89	0.80 ± 0.125	0.58 ± 0.08
5	3e	53.12 ± 3.87	38.92 ± 5.46	67.34 ± 6.19	1.27 ± 0.028	1.73 ± 0.03
6	3f	18.87 ± 1.89	22.36 ± 2.11	54.89 ± 3.12	2.90 ± 0.14	2.45 ± 0.08
7	3g	54.32 ± 2.59	47.89 ± 1.34	71.34 ± 2.19	1.31 ± 0.021	1.48 ± 0.013
8	3h	11.34 ± 2.11	13.01 ± 2.98	52.12 ± 3.17	4.59 ± 0.71	4.00 ± 0.54
9	3i	39.32 ± 1.87	54.68 ± 5.66	62.11 ± 8.76	1.57 ± 0.15	1.13 ± 0.04
10	3j	31.56 ± 2.91	37.65 ± 4.89	89.77 ± 6.77	2.84 ± 0.06	2.38 ± 0.09
11	3k	32.65 ± 1.80	44.41 ± 1.90	40.61 ± 2.10	1.24 ± 0.01	0.91 ± 0.08
12	3l	33.38 ± 3.22	56.77 ± 2.11	44.87 ± 4.65	1.34 ± 0.01	0.79 ± 0.05
13	3m	22.38 ± 4.22	25.92 ± 3.11	79.88 ± 2.55	3.56 ± 0.69	3.08 ± 0.24
14	3n	36.78 ± 2.89	51.98 ± 2.19	64.81 ± 8.54	1.76 ± 0.02	1.25 ± 0.10
15	3o	24.87 ± 4.32	32.11 ± 2.32	57.66 ± 3.18	2.31 ± 3.18	1.79 ± 0.02
16	3p	28.87 ± 2.13	46.43 ± 3.56	61.34 ± 4.97	2.12 ± 0.01	1.32 ± 0.01
17	3q	61.23 ± 1.95	59.88 ± 6.75	88.11 ± 7.28	1.43 ± 0.07	1.47 ± 0.04
18	3r	32.11 ± 2.18	49.76 ± 3.66	62.11 ± 8.21	1.93 ± 0.13	1.24 ± 0.08
19	3s	31.20 ± 2.11	58.46 ± 3.18	53.21 ± 7.65	1.70 ± 0.13	0.91 ± 0.08
20	3t	32.18 ± 3.42	49.88 ± 4.56	65.43 ± 5.89	2.03 ± 0.04	1.31 ± 0.00
21	3u	14.11 ± 4.13	26.28 ± 5.87	51.98 ± 3.98	3.68 ± 1.12	1.97 ± 0.23
22	3v	20.11 ± 1.32	33.68 ± 2.87	43.41 ± 4.13	2.16 ± 0.05	1.29 ± 0.01
23	3w	29.43 ± 2.08	55.42 ± 5.98	49.77 ± 6.89	1.69 ± 0.12	0.89 ± 0.03
24	ETOPOSIDE	27.88 ± 4.32	39.63 ± 3.21	45.31 ± 2.11	1.63 ± 0.20	1.14 ± 0.04

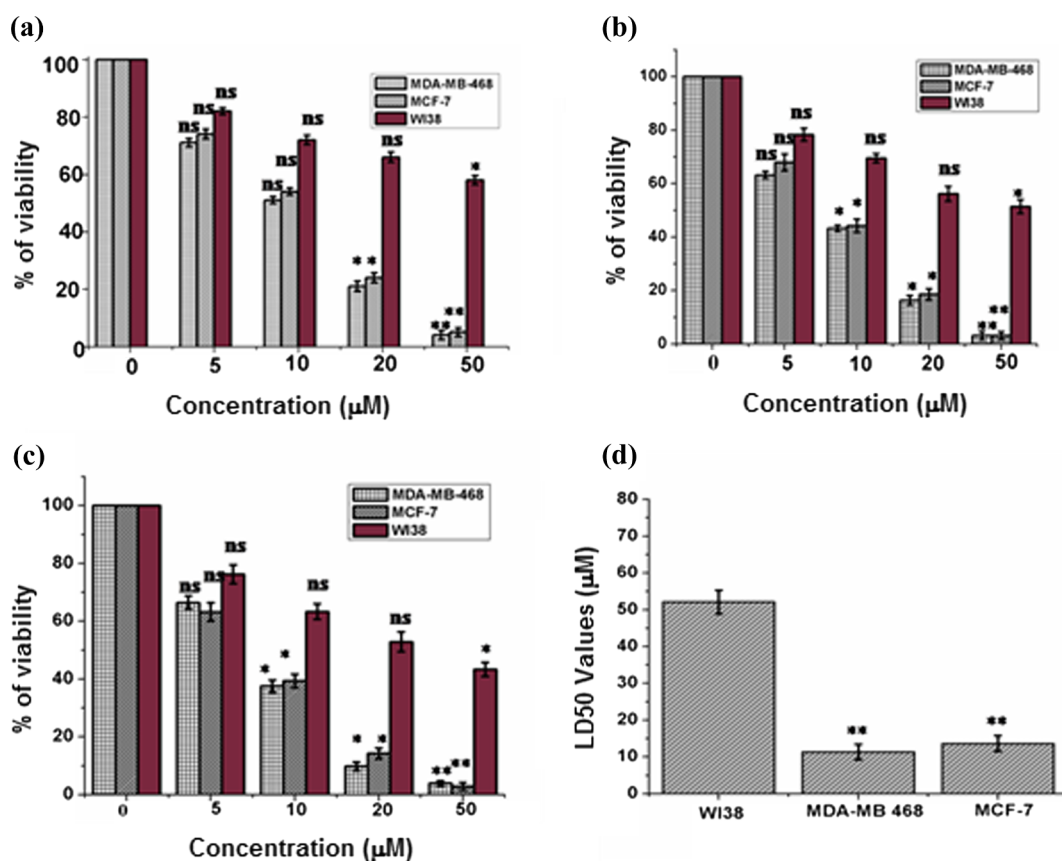


Fig. 1. Assessment of dose dependent cytotoxicity of compound **3h** on triple negative breast cancer cell lines, MDA-MB-468, MCF-7 and WI38 (non-cancer cells) for 24 h (panel A); 48 h (panel B) and 72 h (panel C). (D) LD₅₀ values of compound **3h** on triple negative breast cancer cell lines, MDA-MB-468, MCF-7 and WI38 (non-cancer cells). The data is the average of three experiments ± SD. * = represents P value < 0.05, ** = represents P value < 0.01.

The cancer cells were treated with varying doses (0, 5, 10 and 15 μM) of compound **3h** for 12 h followed by 30 min DCFDA (100 μM) staining and carried out microscopic analysis. The photomicrographs demonstrated a concentration dependent increase in the intensity of the green color in response to compound **3h**, which suggested significant

generation of ROS was induced by compound **3h** in MDA-MB-468 and MCF-7 cells as shown in Fig. 3.

Since ROS plays critical role in changing the mitochondrial permeability transition (MPT), the effect of compound **3h** on mitochondrial damage has been investigated by JC-1 staining which showed a

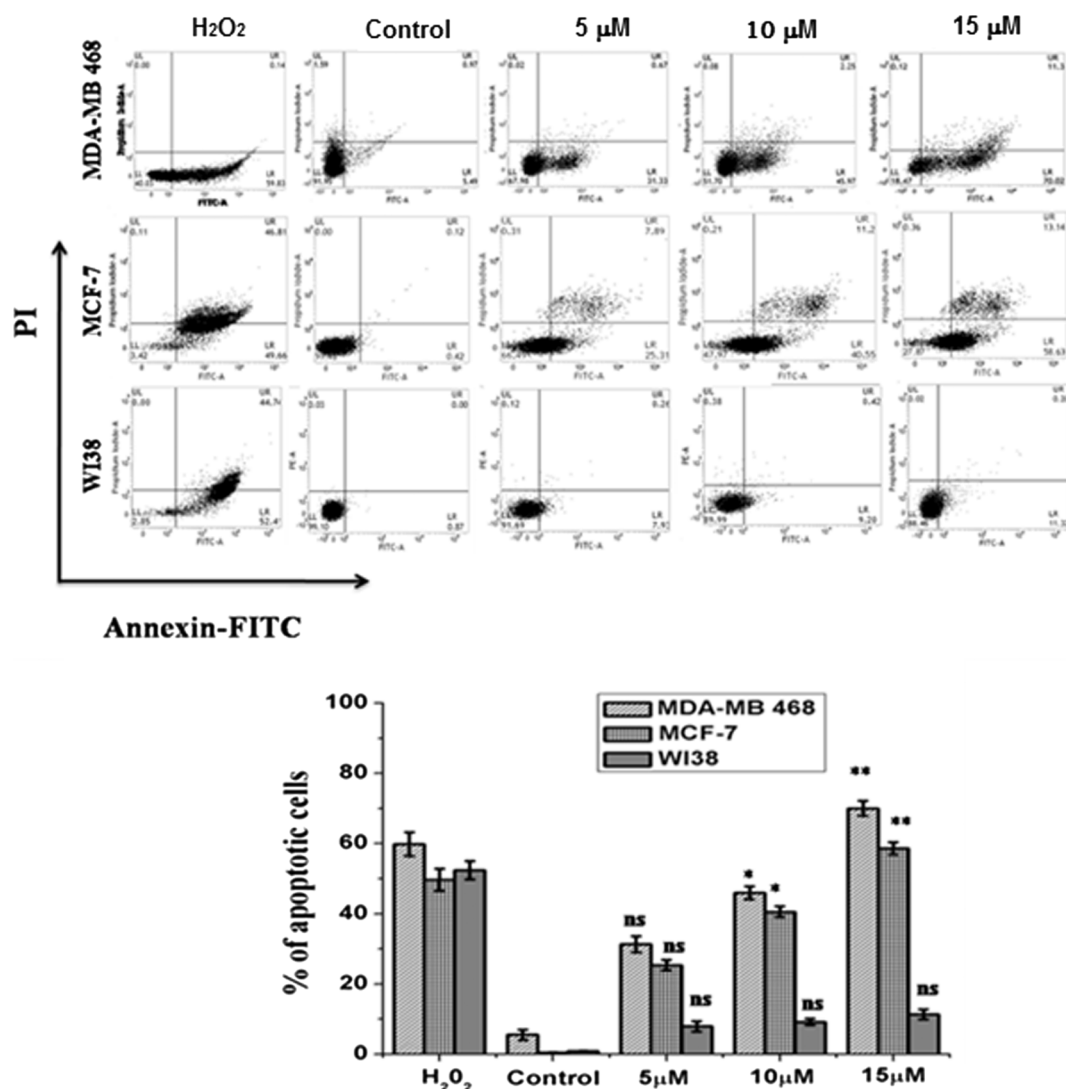


Fig. 2. The dot plot of Annexin V-FITC/PI for the evaluation of apoptosis in MDA-MB 468 and MCF-7 and WI38 (non-cancer cells) treated with the compound **3h**. 1% H₂O₂ has been used as positive control. The data is the average of three experiments \pm SD. * = represents P value < 0.05, ** = represents P value < 0.01.

drastic alteration of the redox status of the cellular mitochondria in response to compound **3h** in a concentration and time dependent manner (Fig. 4). The shift of fluorescence from red to green or a decrease in the red/green ratio indicated the increase in the mitochondrial permeability in response to compound **3h**. Altogether these results imply that compound **3h** mediated generation of ROS may have decisive role in the mitochondrial permeability transition (MPT).

2.2.3. DNA fragmentation in cancer cells mediated by compound **3h**

Earlier reports demonstrated that ROS generation and change in MPT are directly linked with DNA damage and apoptosis, which is an imperative process that controls cellular growth [56]. The association of DNA fragmentation in apoptosis mediated by compound **3h** has also been studied. Firstly, the DAPI staining was done to study apoptotic nuclear morphology of MDA-MB 468 and MCF-7 cells after treatment with compound **3h** at different doses (0, 5, 10 and 15 μ M) for 12 h. The untreated cells did not show any shrinking of nucleus or polynuclear fragmentation whereas the polynuclear fragmentation and shrinking of nucleus was clearly observed in the treated cells (Fig. 5).

The quantitative analysis also confirmed around 70% and 58% apoptotic cells in MDA-MB-468 and MCF-7 cells at 15 μ M respectively which were highly significant compared to the corresponding control cells (5% and 6% respectively) as mention in Fig. 5. Since compound **3h**

mediates the generation of ROS and induces DNA damage in the cancer cells, Comet Assay [57] was performed using MDA-MB-468 and MCF-7 cells to assess DNA damage in response to compound **3h**. It was observed that the fluorescence is confined mostly to the nucleus because of the undamaged DNA in control cells whereas, negatively charged DNA fragments were released from the nucleus and migrated towards the anode leading to a prolonged tail formation in compound **3h** treated cells due to DNA damage. It was further observed that upon treatment with compound **3h** at concentration (at 15 μ M) for 24 h, the tail lengths were 76 ± 1.11 nm and 81 ± 1.54 nm respectively. The increase of tail length is an indication of DNA damage in cells resulting from the treatment of untreated cells which had no or negligible tail length (Fig. 6).

In addition to the earlier mentioned microscopic analysis, the western blot analyses [58] of different apoptotic proteins in MDA-MB-468 and MCF-7 cells were carried out after treatment with compound **3h**. The increase in the expression of pro-apoptotic protein Bax was observed whereas the expression of anti-apoptotic protein Bcl-2 was decreased significantly both in MDA-MB-468 as well as in MCF-7 cells treated with compound **3h** at 15 μ M dose. Moreover, treatment with compound **3h** showed cleavage mediated activation of caspase 3, which suggested caspase mediated apoptosis. Therefore, altogether these results suggest that change in Bax/Bcl-2 ratio as well as caspase 3 plays a

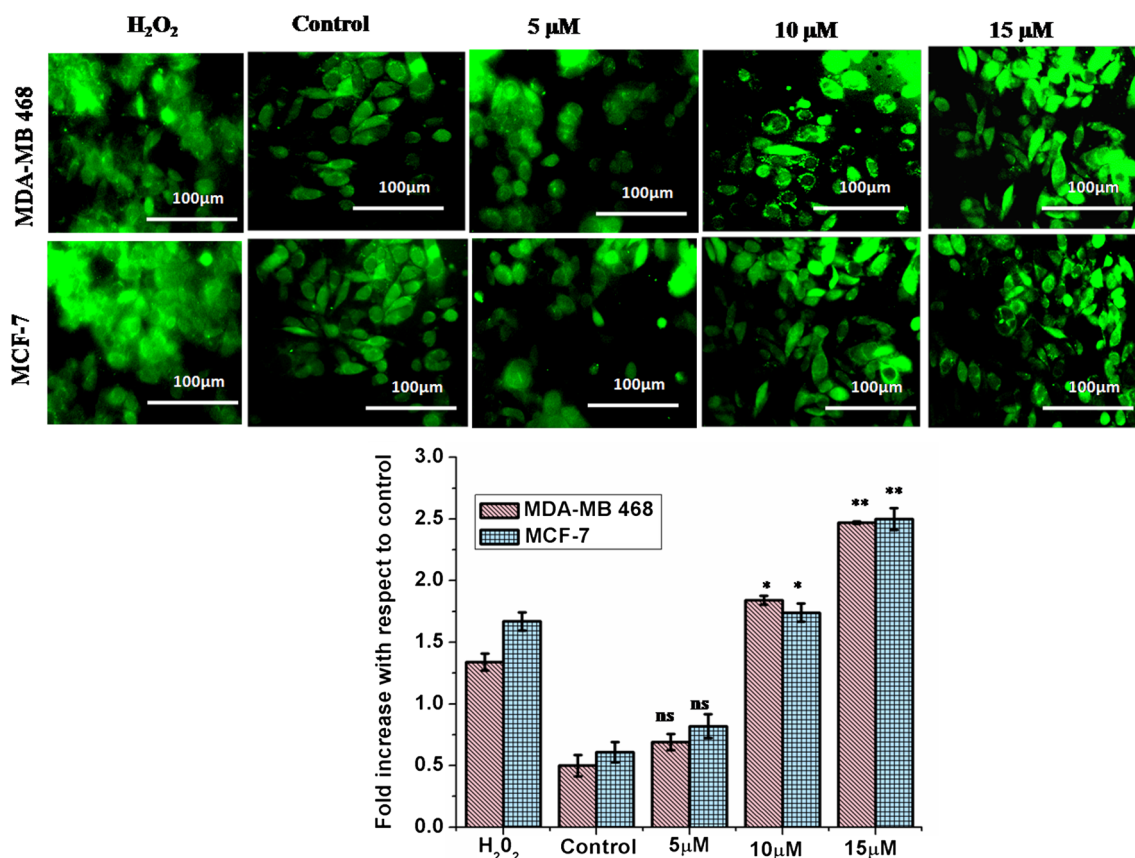


Fig. 3. Fluorescence microscopic image of cells treated with compound **3h** and spectrophotometric fluorescence intensity of the dose-dependent generation of cellular ROS using DCFDA assay. 1% H₂O₂ has been used as positive control. The data is the average of three experiments \pm SD. * = represents P value < 0.05, ** = represents P value < 0.01.

critical role in compound **3h** mediated apoptosis of cancer cells (Fig. 7).

2.2.4. *In silico* studies on the binding interaction of selected compounds with caspase-3 enzyme

In present study, molecular docking was performed to explain the structure activity relationship (SAR) through the correlation in between the biological activity of selected active compounds (compound **3f**, **3h** and **3u**) and their binding affinities towards the active domain of caspase-3 enzyme. It is clear that hydrogen bond interaction with the binding pocket of caspase-3 enzyme play an essential role for their caspase-3 inhibitory activity (Fig. 8). However, during docking study Gibbs free energy (ΔG) indicates that π - π stacking and CH- π hydrophobic interactions with surrounding amino acids (i.e. Tyr 204, Trp 206, Arg 207 and Phe 256) of the binding site are also crucial to increase the biological activity (Table 5, Fig. 8). The 3D docked conformations of compound **3h** and compound **3u** showed the importance of the presence of *p*-methoxybenzyl group at two side arms of the core moiety respectively. This group is used to provide common π - π stacking hydrophobic as well as H-bond interactions with Phe 256 and Ser 251 of caspase-3 enzyme (compound **3h**, $\Delta G = -8.65$ kcal/mol, LD₅₀: 11.34 ± 2.11 ; compound **3u**, $\Delta G = -8.19$ kcal/mol, LD₅₀: 14.11 ± 4.13). Furthermore, additional π - π stacking interaction of compound **3h** with Arg 207 induces its better potential activity against the enzyme. Absence of aromatic groups in compound **3f** clearly specifies its lower binding affinity towards the enzyme which makes a direct correlation with their anti-cancer activity ($\Delta G = -7.57$ kcal/mol, LD₅₀: 18.87 ± 1.89). In addition, Fig. 8 also specified the individual superimposed structures of selected compounds **3f**, **3h** and **3u** along with the co-crystal ligand of PDB ID: 1GFW. This study may provide information regarding the accurate binding pose required for

better inhibitory activity against caspase-3 enzyme. In this case, compound **3f** superimposed only with one part (indoline-2,3-dione group) of the co-crystal ligand whereas, compound **3u** superimposed with the another part (ethoxybenzene group) of the co-crystal ligand. Therefore, compound **3f** and **3u** showed reduced antagonistic activity due to lacking for hydrophobic interactions with two important amino acids i.e. Thr 62 and Ser 65. However, compound **3h** covered up the whole co-crystal ligand moiety after superimposition and showed its binding affinity towards important amino acids of the binding pocket (Table 5). These superimposed structures give significant information to compare their anti-cancer activity.

3. Conclusion

In summary, a series of alkyl/arylsulfonyl sulfoxide derivatives (allicin analogs) were prepared using a generalized reaction condition in satisfactory yield. In addition, some selenium containing analogs have also been prepared in good yield. The synthesized compounds (**3a-w**) were evaluated against cancer cells (MDA-MB-468 and MCF-7 cells) and non-cancer cells (WI38). Four compounds (**3f**, **3h**, **3m** and **3u**) were found promising in terms of the cytotoxic activities against cancer cells and less cytotoxicity against non-cancer cells (WI38). Among four active compounds, compound **3h** has been considered as the best based on the selectivity index. A number of microscopic experiments and fluorescence studies confirmed that compound **3h** exhibits anti-cancer activities against several cancer cells following apoptotic pathway. A docking study has also been carried out to establish the structure-activity relationship of the active compounds.

4. Experimental

4.1. General methods

All reactions were monitored by thin layer chromatography over silica gel coated TLC plates. Silica gel 230–400 mesh was used for column chromatography. ^1H and ^{13}C NMR spectra were recorded on a Bruker Avance 500 MHz spectrometer using CDCl_3 as solvent and TMS as the internal reference unless stated otherwise. Chemical shift values are expressed in δ ppm. ESI-MS were recorded on a Micromass mass spectrometer. Elementary analysis was carried out on a Carlo Erba analyzer. Biological experiments were carried out in a Shimadzu UV-2401PC spectrophotometer. Commercially available grades of organic solvents of adequate purity were used in many reactions.

Breast cancer cell lines- MDA-MB-468, MCF-7 (human breast cancer cells), and WI38 (human lung fibroblast) cells were obtained from the central cell repository of National Center for Cell Science (NCCS), Pune, India and cultured as suggested by the supplier. All the above cell lines were cultured either in RPMI 1640 or DMEM, containing 10% FBS, 1 mM sodium pyruvate, 2 mM L-glutamine, non-essential amino acids, 100 units/L penicillin, 100 mg/L streptomycin and 50 mg/L gentamycin sulfate at 37°C with 5% CO_2 .

The cell culture media along with ingredients were purchased from

HiMedia (India). FBS was procured from Gibco (USA). DMSO was purchased from SRL (India). An annexin V-FITC apoptosis assay kit was bought from BD Bioscience (India). A Caspase 3 Assay Kit (ab39401) and Human Apoptosis Array Kit were purchased from AbCam (UK) and R&D Systems (USA), respectively.

4.1.1. General experimental condition for the preparation of alkyl/arylsulfonyl sulfoxide derivatives (allicin analogs)

To a solution of disulfide derivatives (**2a-s**) (1.0 mmol) in CH_2Cl_2 (3 mL) was added *m*-chloroperbenzoic acid (1.0 mmol) in CH_2Cl_2 (2 mL) at -20°C and the reaction mixture was stirred at the same temperature for appropriate time (Table 2). The reaction mixture was poured into water and extracted with CH_2Cl_2 (2×25 mL) and organic layer was washed with satd. aq. NaHCO_3 . The combined organic layers were dried over Na_2SO_4 , filtered and concentrated under reduced pressure. The crude product was purified over SiO_2 using hexane-EtOAc (1:2) as eluant to give the pure products (Table 2).

4.1.2. General experimental condition for the preparation of selenenyl selenoxide derivatives

To the solution of diselenide derivative (1.0 mmol) in CH_2Cl_2 (5 mL) were added NaIO_4 (1.0 mmol) and TBAB (0.2 mmol) in water (1 mL) at room temperature and the reaction mixture was stirred at the same

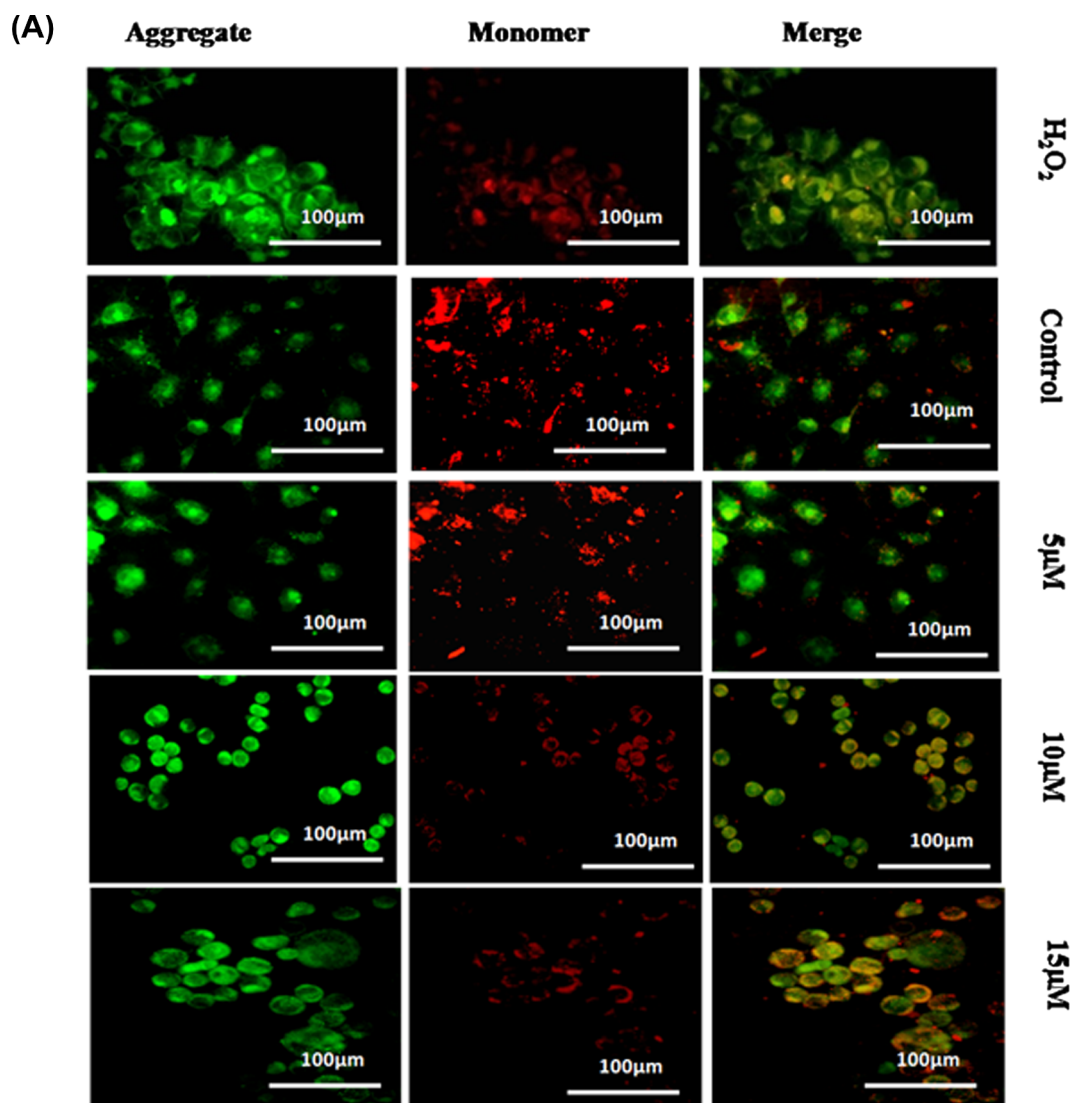


Fig. 4. Dose dependent mitochondrial membrane potential by JC1 staining of (A) MDA-MB 468 cells and (B) MCF-7 cells treated with compound **3h**. 1% H_2O_2 has been used as positive control.

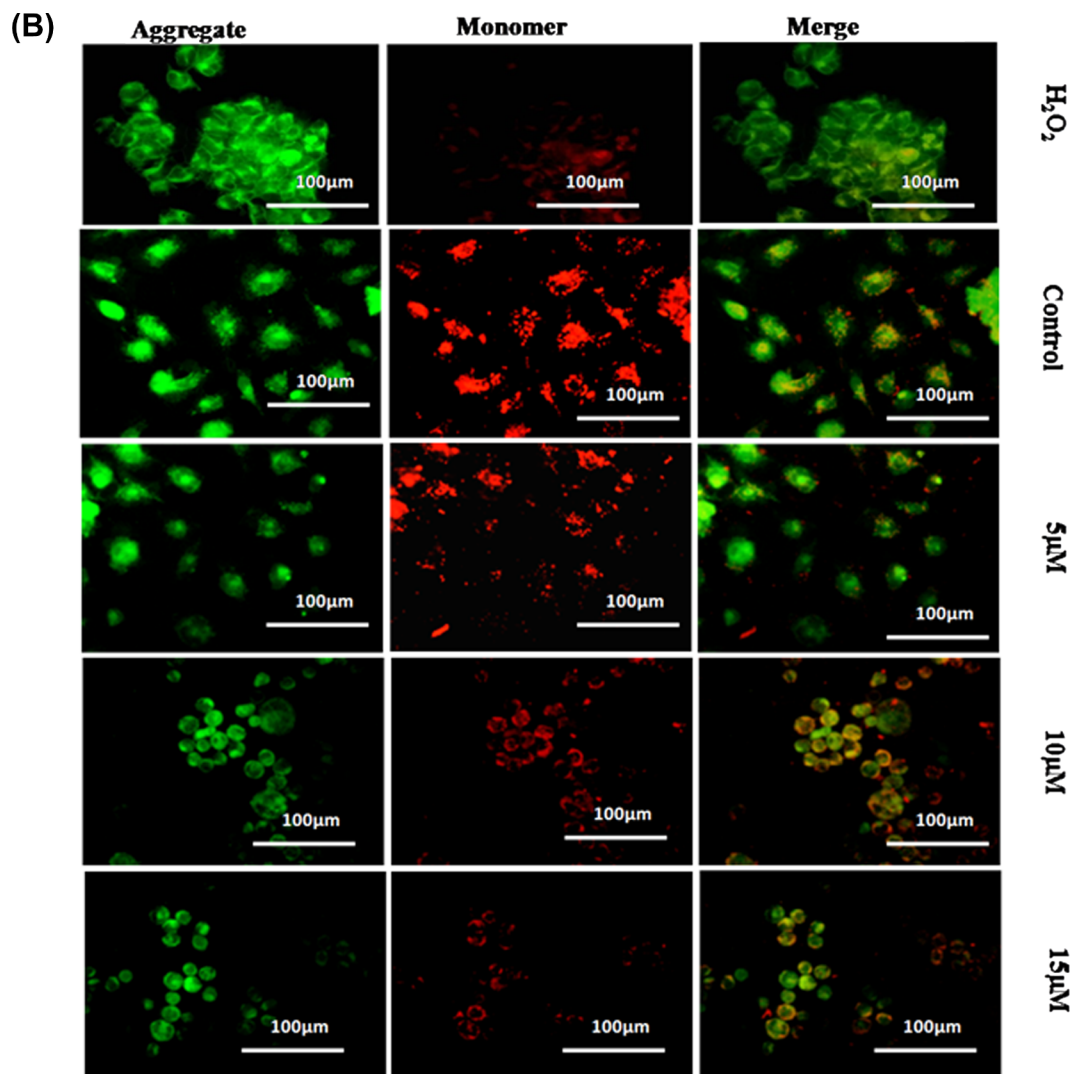


Fig. 4. (continued)

temperature for appropriate time (Table 3). The reaction mixture was poured into water and extracted with CH₂Cl₂ (2 × 25 mL) and organic layer was washed with satd. aq. NaHCO₃. The combined organic layers were dried over Na₂SO₄, filtered and concentrated under reduced pressure. The crude product was purified over SiO₂ using hexane-EtOAc (1:2) as eluant to give the pure selenenyl selenoxide derivative (Table 3).

4.2. Spectral data of synthesized compounds

4.2.1. *S*-propyl propane-1-sulfinothioate (3a)

Colorless oil; ¹H NMR (500 MHz, CDCl₃): δ 3.19–3.02 (m, 4H, 2 SCH₂), 1.96–1.65 (m, 4H, 2CH₂), 1.10, 1.05 (2 t, *J* = 7.5 Hz each, 2 × 3H, 2CH₃); ¹³C NMR (125 MHz, CDCl₃): δ 57.9 (1C), 41.1 (1C), 24.4 (1C), 17.3 (1C), 13.2 (2C); *m/z*: 167.0 [M + 1]⁺; Anal. Calcd. for C₆H₁₄OS₂ (166.30): C, 43.33; H, 8.49; found: C, 43.18; H, 8.60.

4.2.2. *S*-isopropyl propane-2-sulfinothioate (3b)

Colorless oil; ¹H NMR (500 MHz, CDCl₃): δ 2.91–2.89 (m, 2H), 1.05–1.02 (2 t, *J* = 5.5 Hz each, 12H, 4 CH₃); ¹³C NMR (125 MHz, CDCl₃): δ 28.2 (2 CH), 21.8 (4 CH₃); *m/z*: 167.0 [M + 1]⁺; Anal. Calcd. for C₆H₁₄OS₂ (166.30): C, 43.33; H, 8.49; found: C, 43.17; H, 8.60.

4.2.3. *S*-butyl butane-1-sulfinothioate (3c)

Colorless oil; ¹H NMR (500 MHz, CDCl₃): δ 3.17–3.08 (m, 4H),

1.81–1.71 (m, 4H), 1.48–1.37 (m, 4H), 0.94–0.86 (2 t, *J* = 5.5 Hz each, 6H, 2CH₃); ¹³C NMR (125 MHz, CDCl₃): δ 55.9 (1C), 32.8, 32.5 (2C), 25.4 (1C), 21.7, 21.5 (2C), 10.3 (2C); *m/z*: 195.0 [M + 1]⁺; Anal. Calcd. for C₈H₁₈OS₂ (194.35): C, 49.44; H, 9.33; found: C, 49.26; H, 9.50.

4.2.4. *S*-3-methylbut-2-enyl 3-methylbut-2-ene-1-sulfinothioate (3d)

Colorless oil; ¹H NMR (500 MHz, CDCl₃): δ 5.01–4.88 (m, 4H), 3.58–3.48 (m, 2H), 3.31–3.21 (m, 2H), 1.78 (2 s, 6H, 2CH₃); ¹³C NMR (125 MHz, CDCl₃): δ 115.7, 115.3 (2C = C, 4C), 46.4 (2CH₂), 21.0, 20.9 (2CH₃); *m/z*: 219.0 [M + 1]⁺; Anal. Calcd. for C₁₀H₁₈OS₂ (218.37): C, 55.00; H, 8.31; found: C, 54.83; H, 8.50.

4.2.5. *S*-tetradecyl tetradecane-1-sulfinothioate (3e)

White solid; m.p. 54–55 °C (EtOH); ¹H NMR (500 MHz, CDCl₃): δ 3.19–3.06 (m, 2H), 1.86–1.59 (m, 2H), 1.48–1.20 (m, 48H), 0.88 (t, *J* = 5.5 Hz each, 6H, 2 CH₃); ¹³C NMR (125 MHz, CDCl₃): δ 56.3 (1C), 32.9–28.6 (24C), 23.5 (1C), 22.7 (1C), 14.1 (1C); *m/z*: 475.3 [M + 1]⁺; Anal. Calcd. for C₂₈H₅₈OS₂ (474.88): C, 70.82; H, 12.31; found: C, 70.67; H, 12.48.

4.2.6. *S*-2-acetoxyethyl 2-acetoxyethanesulfinothioate (3f)

Colorless oil; ¹H NMR (500 MHz, CDCl₃): δ 4.61–4.32 (m, 4H), 3.48–3.34 (m, 4H), 2.09 (s, 3H); ¹³C NMR (125 MHz, CDCl₃): δ 63.2 (1C), 57.5 (1C), 54.9 (1C), 33.7 (1C), 20.7 (2C); *m/z*: 255.0 [M + 1]⁺;

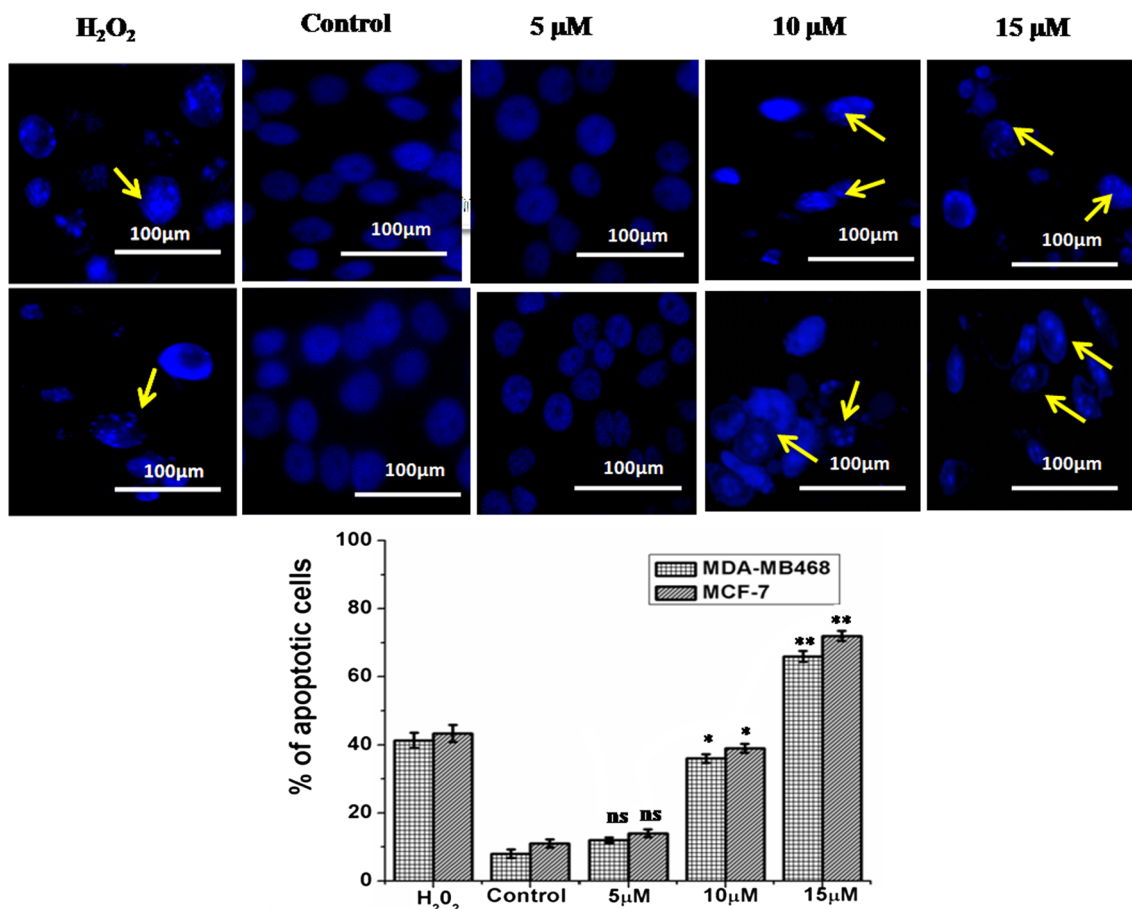


Fig. 5. The treatment with compound **3h** induces apoptosis in MDA-MB 468 and MCF-7 cells as is depicted in cellular morphology study by DAPI staining. The arrows indicate the polynuclear fragmentation and shrinking of nucleus. 1% H₂O₂ has been used as positive control. The data is the average of three experiments \pm SD. * = represents P value < 0.05, ** = represents P value < 0.01.

Anal. Calcd. for C₈H₁₄O₅S₂ (254.32): C, 37.78; H, 5.55; found: C, 37.61; H, 5.70.

4.2.7. *S*-benzyl phenylmethanesulfinothioate (**3g**)

Colorless oil; ¹H NMR (500 MHz, CDCl₃): δ 7.38–7.25 (m, 10H, Ar-H), 4.34–4.24 (2 ABq, J = 13.0 Hz each, 4H, 2 PhCH₂); ¹³C NMR (125 MHz, CDCl₃): δ 136.5–127.6 (Ar-C), 62.1 (1C), 36.0 (1C); m/z : 263.0 [M + 1]⁺; Anal. Calcd. for C₁₄H₁₄OS₂ (262.39): C, 64.08; H, 5.38; found: C, 63.95; H, 5.50.

4.2.8. *S*-*p*-methoxybenzyl (*p*-methoxyphenyl)methanesulfinothioate (**3h**)

Colorless oil; ¹H NMR (500 MHz, CDCl₃): δ 7.27–7.19 (m, 4H, Ar-H), 6.84 (d, J = 10.5 Hz, 2H, Ar-H), 6.81 (d, J = 8.5 Hz, 2H, Ar-H), 4.29–4.19 (2 dd, J = 7.5, 4.5 Hz each, 4H, 2 CH₂), 3.82, 3.78 (2 s, 6H, 2 OCH₃); ¹³C NMR (125 MHz, CDCl₃): δ 132.0–114.2 (Ar-C), 61.5 [S (O)CH₂], 55.2 (2 OCH₃), 35.7 (SCH₂); m/z : 323.0 [M + 1]⁺; Anal. Calcd. for C₁₆H₁₈O₃S₂ (322.44): C, 59.60; H, 5.63; found: C, 59.44; H, 5.78.

4.2.9. *S*-(naphthalen-2-yl)methyl (naphthalen-2-yl)methanesulfinothioate (**3i**)

Colorless oil; ¹H NMR (500 MHz, CDCl₃): δ 7.85–7.72 (m, 7H, Ar-H), 7.53–7.41 (m, 7H, Ar-H), 4.45–4.26 (m, 4H); ¹³C NMR (125 MHz, CDCl₃): δ 134.5–126.1 (Ar-C), 62.7 (1C), 45.5 (1C); m/z : 363.0 [M + 1]⁺; Anal. Calcd. for C₂₂H₁₈OS₂ (362.50): C, 72.89; H, 5.00; found: C, 72.72; H, 5.16.

4.2.10. *S*-4-(*p*-methoxyphenoxy)butyl 4-(*p*-methoxyphenoxy)butane-1-sulfinothioate (**3j**)

Colorless oil; ¹H NMR (500 MHz, CDCl₃): δ 6.80–6.78 (m, 8H, Ar-H), 4.44 (t, J = 6.0 Hz, 4H, 2CH₂), 3.97 (t, J = 6.0 Hz, 4H, 2CH₂), 3.78 (s, 6H, 2 OCH₃), 2.01–1.99 (m, 8H, 4 CH₂); ¹³C NMR (125 MHz, CDCl₃): δ 133.7–114.6 (Ar-C), 76.9 (2C), 67.7 (2C), 55.6 (2C), 25.8 (2C), 24.6 (2C); m/z : 453.1 [M + 1]⁺; Anal. Calcd. for C₂₃H₃₂O₅S₂ (452.62): C, 61.03; H, 7.13; found: C, 60.87; H, 7.26.

4.2.11. *S*-2-(2,3,4,6-tetra-*O*-acetyl- β -D-galactopyranosyl)ethyl 2-(2,3,4,6-tetra-*O*-acetyl- β -D-galactopyranosyl)ethane-1-sulfinothioate (**3k**)

This compound is obtained as mixture of two regio-isomers, spectral value of major isomer is given below.

White solid; m.p. 57–58 °C [EtOH]; ¹H NMR (500 MHz, CDCl₃): δ 5.37 (br s, 2H, 2H-4), 5.18 (t, J = 9.0 Hz, 2H, 2H-2), 5.01 (t, J = 9.0 Hz, 2H, 2H-3), 4.58–4.50 (2 d, J = 9.0 Hz, 2H, 2H-1), 4.30–4.25 (m, 1H, 1 OCH), 4.21–4.09 (m, 5H, 2H-6_{ab}, 1 OCH), 4.07–3.87 (m, 1H, 1 OCH), 3.87–3.90 (m, 2H, 2H-5), 3.89–3.81 (m, 1H, 1 OCH), 3.41–3.30 (m, 4H, 2 SCH₂), 2.19–1.99 (4 s, 24H, 4 OCOCH₃); ¹³C NMR (125 MHz, CDCl₃): δ 170.2–169.1 (OCOCH₃), 101.5–101.1 (4 C-1, 2 regioisomer), 70.9 (4 C), 69.1 (2 C), 68.7 (2 C), 68.5 (2 C), 67.0 (2 C), 63.0 (2 C, SCH₂), 62.7 (2 C, 61.1 (2 C, OCH₂), 56.0, 55.8 (2 C, SCH₂), 20.8–20.5 (OCOCH₃); m/z : 853.1 [M + Na]⁺; Anal. Calcd. for C₃₂H₄₆O₂₁S₂ (830.82): C, 46.26; H, 5.58; found: C, 46.10; H, 5.40.

4.2.12. *S*-2-(2,3,4,6-tetra-*O*-acetyl- β -D-glucopyranoside)ethyl 2-(2,3,4,6-tetra-*O*-acetyl- β -D-glucopyranosyl)ethane-1-sulfinothioate (**3l**)

This compound is obtained as mixture of two regio-isomers, spectral value of major isomer is given below.

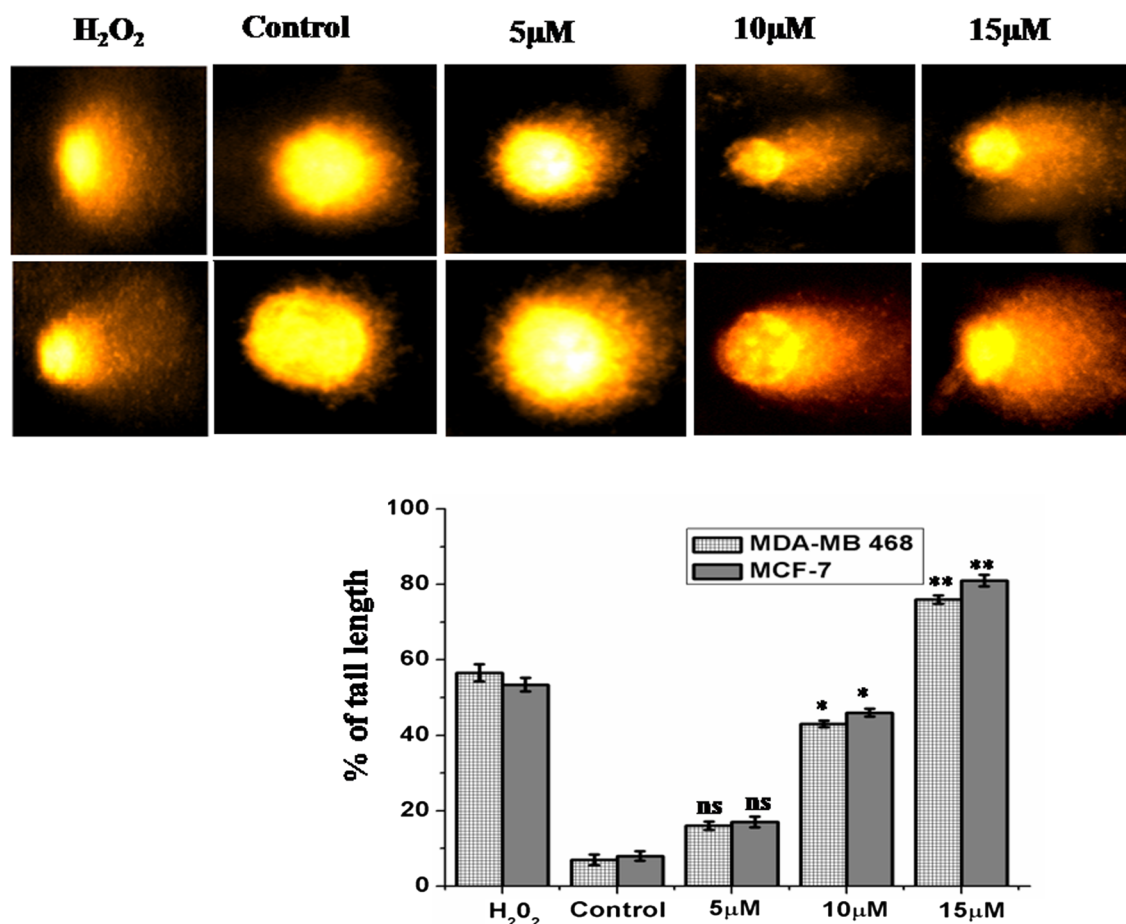


Fig. 6. Comet assay of MDA-MB 468 and MCF-7 cells following treatment with compound **3h** at the doses 5 μ M, 10 μ M and 15 μ M. 1% H₂O₂ has been used as positive control. The data is the average of three experiments \pm SD. * = represents P value < 0.05, ** = represents P value < 0.01.

Colorless oil; ¹H NMR (500 MHz, CDCl₃): δ 5.18 (t, J = 9.0 Hz, 2H, 2H-2), 5.06 (t, J = 8.5 Hz, 2H, 2H-3), 5.00–4.96 (m, 2H, 2H-4), 4.60–4.51 (m, 2H, 2H-1), 4.30–4.09 (m, 6H, 2H-6_{ab}, 2H-5), 4.08–3.79 (m, 2H, OCH₂), 3.75–3.78 (m, 2H, OCH₂), 3.39–3.29 (m, 4H, 2 SCH₂), 2.09–2.00 (4 s, 24H, 4 OCOCH₃); ¹³C NMR (125 MHz, CDCl₃): δ 170.4–169.1 (OCOCH₃), 101.0–100.6 (4 C-1, 2 regio-isomer), 72.7 (4 C-2, 2 regio-isomer), 72.0 (4 C-3, 2 regio-isomer), 71.1 (4 C-4, 2 regio-isomer), 69.2 (4 C-6, 2 regio-isomer), 68.2 (4 C-5, 2 regio-isomer), 63.0 (SCH₂), 61.7 (OCH₂), 55.8 (SCH₂), 20.9–20.5 (OCOCH₃); m/z : 853.1 [M + Na]⁺; Anal. Calcd. for C₃₂H₄₆O₂₁S₂ (830.82): C, 46.26; H, 5.58; found: C, 46.06; H, 5.40.

4.2.13. S-2-(2,3,4-tri-O-acetyl- α -L-rhamnopyranosyl)ethyl 2-(2,3,4-tri-O-acetyl- α -L-rhamnopyranosyl)ethane-1-sulfinothioate (3m)

This compound is obtained as mixture of two regio-isomers, spectral value of major isomer is given below.

Colorless oil; ¹H NMR (500 MHz, CDCl₃): δ 5.29–5.21 (m, 4H, 2 H-1, 2 H-2), 5.07–5.01 (m, 2 H, 2 H-4), 4.80–4.78 (m, 2 H, 2 H-3), 4.25–4.16 (m, 2 H, 2 H-5), 4.05–3.78 (m, 4H 2 OCH₂), 3.44–3.32 (m, 4H, 2 SCH₂), 2.15–1.96 (4 s, 24H, 4 OCOCH₃), 1.28–1.22 (m, 6 H, 2 CH₃); ¹³C NMR (125 MHz, CDCl₃): δ 169.9–169.7 (OCOCH₃), 97.8–97.5 (4 C-1, 2 regio-isomer), 71.0–70.7 (4 C-2, 2 regio-isomer), 69.6–69.5 (4 C-3, 2 regio-isomer), 69.0–68.9 (4 C-4, 2 regio-isomer), 67.7–67.3 (OCH₂, 2 regio-isomer), 66.9–66.8 (4 C-5, 2 regio-isomer), 60.3 (OCH₂, 2 regio-isomer), 55.4–55.3 (SCH₂, 2 regio-isomer), 32.7 (SCH₂, 2 regio-isomer), 21.0–20.7 (OCOCH₃), 17.4 (CCH₃); m/z : 737.1 [M + Na]⁺; Anal. Calcd. for C₂₈H₄₂O₁₇S₂ (714.75): C, 47.05; H, 5.92; found: C, 46.86; H, 6.10.

4.2.14. S-phenyl benzenesulfinothioate (3n)

Colorless oil; ¹H NMR (500 MHz, CDCl₃): δ 7.60–7.21 (m, 10H, Ar-H); ¹³C NMR (125 MHz, CDCl₃): δ 143.0–127.2 (Ar-C); m/z : 235.0 [M + 1]⁺; Anal. Calcd. for C₁₂H₁₀OS₂ (234.33): C, 61.50; H, 4.30; found: C, 61.37; H, 4.50.

4.2.15. S-p-tolyl 4-methylbenzenesulfinothioate (3o)

Colorless oil; ¹H NMR (500 MHz, CDCl₃): δ 7.80–7.09 (m, 8H, Ar-H), 2.42, 3.38 (2 s, 6H, 2 CH₃); ¹³C NMR (125 MHz, CDCl₃): δ 144.6–124.6 (Ar-C), 21.6–21.1 (2 CH₃); m/z : 263.0 [M + 1]⁺; Anal. Calcd. for C₁₄H₁₄OS₂ (262.39): C, 64.08; H, 5.38; found: C, 63.92; H, 5.55.

4.2.16. S-4-nitrophenyl 4-nitrobenzenesulfinothioate (3p)

Colorless oil; ¹H NMR (500 MHz, CDCl₃): δ 8.33 (d, J = 9.0 Hz, 2H, Ar-H), 8.25 (d, J = 9.0 Hz, 2H, Ar-H), 7.81 (d, J = 9.0 Hz, 2H, Ar-H), 7.63 (d, J = 9.0 Hz, 2H, Ar-H); ¹³C NMR (125 MHz, CDCl₃): δ 147.9–124.5 (Ar-C); m/z : 325.9 [M + 1]⁺; Anal. Calcd. for C₁₂H₈N₂O₅S₂ (324.33): C, 44.44; H, 2.49; found: C, 44.28; H, 2.65.

4.2.17. S-naphthalen-2-yl naphthalene-2-sulfinothioate (3q)

White solid; m.p. 93–94 °C (EtOH); ¹H NMR (500 MHz, CDCl₃): δ 7.94–7.12 (m, 14H, Ar-H); ¹³C NMR (125 MHz, CDCl₃): δ 139.7–122.4 (Ar-C); m/z : 335.0 [M + 1]⁺; Anal. Calcd. for C₂₀H₁₄OS₂ (334.45): C, 71.82; H, 4.22; found: C, 71.70; H, 4.35.

4.2.18. S-pyridin-2-yl pyridine-2-sulfinothioate (3r)

Colorless oil; ¹H NMR (500 MHz, CDCl₃): δ 8.72–8.70 (m, 1H, Ar-H), 8.51–8.49 (m, 1H, Ar-H), 7.93–7.89 (m, 1H, Ar-H), 7.86–7.72 (m, 3H, Ar-H), 7.60–7.50 (m, 1H, Ar-H), 7.39–7.32 (m, 1H, Ar-H); ¹³C NMR

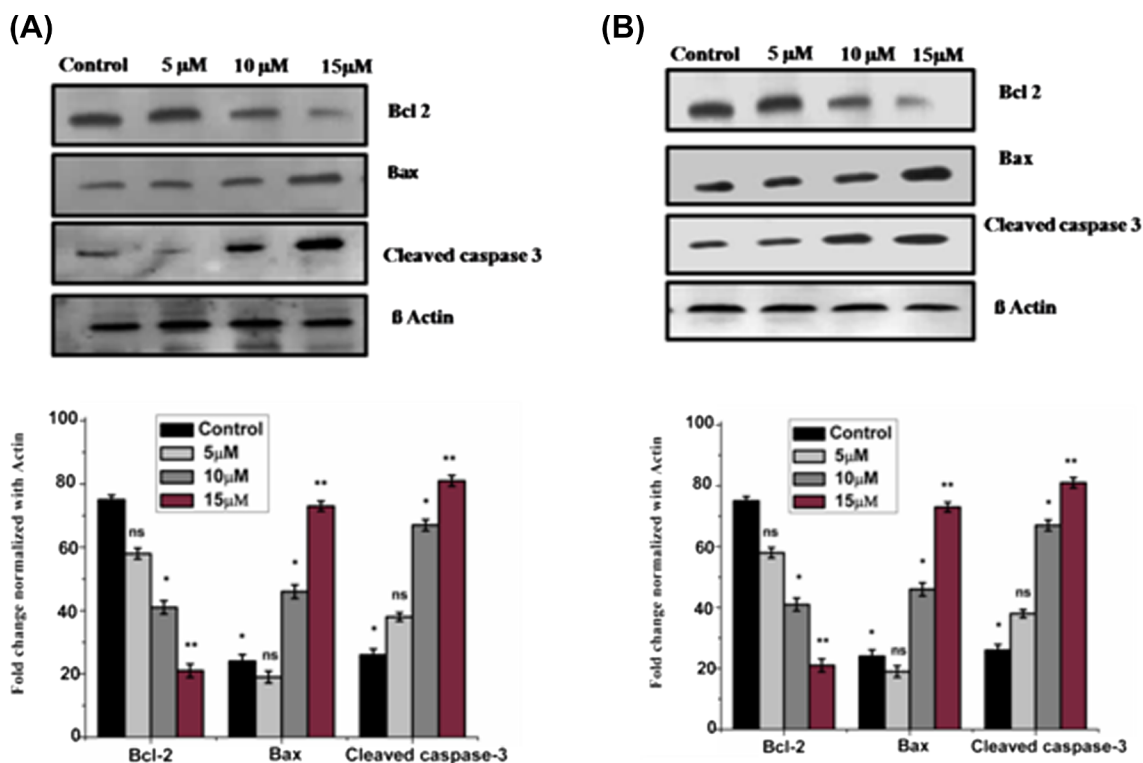


Fig. 7. Western blot analysis of apoptotic proteins like cleaved Caspase-3, Bax and Bcl2 in (a) MDA-MB-468 and (b) MCF-7 suggesting the induction of apoptotic pathway upon treatment of the cells with compound **3h**. The data is the average of three experiments \pm SD. * = represents P value < 0.05, ** = represents P value < 0.01.

(125 MHz, CDCl_3): δ 159.9–119.8 (Ar-C); m/z : 237.0 $[\text{M} + 1]^+$; Anal. Calcd. for $\text{C}_{10}\text{H}_8\text{N}_2\text{OS}_2$ (236.31): C, 50.83; H, 3.41; found: C, 50.70; H, 3.60.

4.2.19. S-1-phenyl-1H-tetrazol-5-yl 1-phenyl-1H-tetrazole-5-sulfinothioate (3s)

Colorless oil; ^1H NMR (500 MHz, CDCl_3): δ 7.75–7.50 (m, 10H, Ar-H); ^{13}C NMR (125 MHz, CDCl_3): δ 140.6–121.2 (Ar-C); m/z : 371.0 $[\text{M} + 1]^+$; Anal. Calcd. for $\text{C}_{14}\text{H}_{10}\text{N}_8\text{OS}_2$ (370.41): C, 45.40; H, 2.72; found: C, 45.25; H, 2.60.

4.2.20. Se-benzyl phenylmethaneseleninoselenoate (3t)

White solid; m.p. 103–104 °C (EtOH); ^1H NMR (500 MHz, D_2O): δ 7.50–7.42 (m, 10H, Ar-H), 4.36–4.17 (m, 4H, 2 CH_2); ^{13}C NMR (125 MHz, D_2O): δ 129.7–127.3 (Ar-C), 59.9 (2 CH_2); m/z : 358.9 $[\text{M} + 1]^+$; Anal. Calcd. for $\text{C}_{14}\text{H}_{14}\text{OSe}_2$ (357.93): C, 47.21; H, 3.96; found: C, 47.10; H, 4.10.

4.2.21. Se-p-methoxybenzyl (p-methoxyphenyl)methaneseleninoselenoate (3u)

Colorless oil; ^1H NMR (500 MHz, CDCl_3): δ 7.31–7.21 (m, 4H, Ar-H), 6.89–6.82 (m, 4H, Ar-H), 5.02 (d, $J = 10.5$ Hz, 1H, SeCH_2), 4.78 (d, $J = 11.5$ Hz, 1H, SeCH_2), 4.63–4.54 (m, 2H, SeCH_2), 3.80 (s, 6H, 2 OCH_3); ^{13}C NMR (125 MHz, CDCl_3): δ 158.7–112.7 (Ar-C), 71.4 (SeCH_2), 63.6 (SeCH_2), 55.5 (2 OCH_3); m/z : 418.9 $[\text{M} + 1]^+$; Anal. Calcd. for $\text{C}_{16}\text{H}_{18}\text{O}_3\text{Se}_2$ (417.95): C, 46.17; H, 4.36; found: C, 46.05; H, 4.50.

4.2.22. Se-(naphthalen-2-yl)methyl (naphthalen-2-yl)methaneseleninoselenoate (3v)

White solid; m.p. 109–110 °C (EtOH); ^1H NMR (500 MHz, CDCl_3): δ 8.00–7.89 (m, 7H, Ar-H), 7.63–7.50 (m, 7H, Ar-H), 4.18–4.10 (m, 4H, 2 SeCH_2); ^{13}C NMR (125 MHz, D_2O): δ 127.7–124.7 (Ar-C), 64.0 (SeCH_2), 63.4 (SeCH_2); m/z : 458.9 $[\text{M} + 1]^+$; Anal. Calcd. for $\text{C}_{22}\text{H}_{18}\text{OSe}_2$

(457.96): C, 57.91; H, 3.98; found: C, 57.80; H, 4.15.

4.2.23. S-phenyl benzeneseleninoselenoate (3w)

White solid; m.p. 128–129 °C (EtOH); ^1H NMR (500 MHz, D_2O): δ 7.79–7.76 (m, 2H, Ar-H), 7.76–7.70 (m, 2H, Ar-H), 7.60–7.49 (m, 6H, Ar-H); ^{13}C NMR (125 MHz, D_2O): δ 132.9–124.5 (Ar-C); m/z : 330.9 $[\text{M} + 1]^+$; Anal. Calcd. for $\text{C}_{12}\text{H}_{10}\text{OSe}_2$ (329.90): C, 43.92; H, 3.07; found: C, 43.80; H, 3.20.

4.3. MTT assay for checking cytotoxicity of compounds

In order to determine the effect of the synthesized compounds on cell proliferation, MTT assay was performed [50,51]. Briefly, MDA-MB-468, MCF-7 and WI38 cells were grown in 96 well plates in presence of the synthesized derivatives (0–50 μM) for 24 h, 48 h and 72 h in 5% FBS containing phenol red free DMEM. The cells were washed thrice with PBS to make them clear from the test agents. MTT (200 μL ; 0.5 mg/mL dissolved in phosphate buffer saline (PBS) having a pH value of 7.4) were added to each well and incubated at 37 °C for 4 h in a humidified incubator containing 5% CO_2 . The purple colored formazan crystals formed in the wells were dissolved in DMSO and absorbance was measured at 570 nm with a microplate reader.

4.4. Apoptotic cell quantification by AnnexinV-FITC staining

Induction of apoptosis was measured by flow cytometry after AnnexinV-FITC/PI staining [53] using BD Bioscience kit. Briefly, post treatment 0.5×10^6 cells with compound **3h** were washed in ice-cold $1 \times$ PBS and resuspended in 100 μL of binding buffer and incubated with 5 μL of annexin V-FITC and 5 μL of PI for 15 min at room temperature in a dark place as per manufacturer's guidelines. Flow cytometric analysis was immediately performed using a FACS Verse instrument (BD).

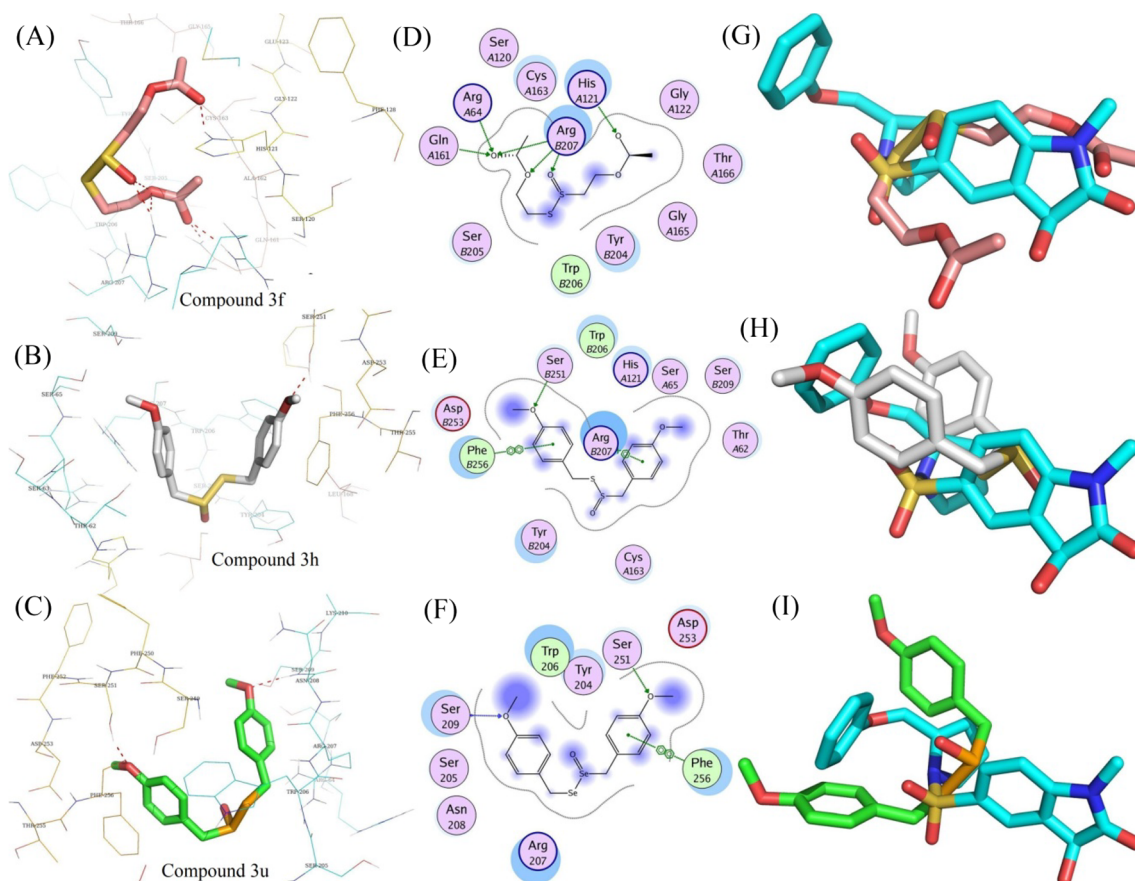


Fig. 8. Molecular docking study of three selected compounds (**3f**, **3h** and **3u**) with caspase-3 enzyme co-crystal (PDB ID: 1GFV). Figure (A), (B) and (C) shows docked conformations of compound **3f** (pink), **3h** (white) and **3u** (green) into the binding pocket of caspase-3. Red dotted lines (---) indicate the H-bond interactions. Figure (D), (E) and (F) pointed out the 2D diagram of compounds **3f**, **3h** and **3u** respectively. Additionally, the superimposed structures of co-crystal ligand (cyan) with all three selected individual molecules are represented by (G), (H) and (I).

4.5. ROS estimation by DCFDA method

Intracellular ROS was measured using DCFDA method [55]. Briefly, MDA-MB-468 and MCF-7, cells were treated with 5 μ M, 10 μ M and 15 μ M doses of compound **3h** for 12 h. After the treatment, the media was discarded and cells were washed thrice with ice cold Hanks balanced salt solution (HBSS) and incubated with DCFDA (100 μ M final) for 30 min at 37 $^{\circ}$ C. Then, cells were lysed with alkaline solutions and fluorescence intensity was measured at excitation of 485 nm and emission at 520 nm (Biotek). The estimation of ROS was measured by both fluorometer as well as by microscope.

4.6. Mitochondrial membrane potential measurement by JC1 staining

Assessment of mitochondrial permeability was measured by JC1 staining as described earlier [55]. Mitochondria depolarization is specifically indicated by JC-1 dye, which is a cationic dye that exhibits potential-dependent accumulation in mitochondria, indicated by a fluorescence emission shift from red to green as the mitochondrial damages and loses its membrane potential. MDA-MB-468 and MCF-7 cells

were treated with 5 μ M, 10 μ M and 15 μ M of compound **3h**. After the treatment, the cells were washed with phosphate buffered saline (PBS) and incubated with (10 μ g/ml) JC-1 for 30 min in dark at 37 $^{\circ}$ C. Finally images were captured under a fluorescent microscope (Leica, Wetzlar, Germany).

4.7. Apoptotic nuclear morphology study by DAPI staining

Nuclear morphology of MDA-MB-468 and MCF-7 cells was studied by DAPI staining. After exposure of compound **3h** (5 μ M, 10 μ M and 15 μ M) for 12 h, cells were washed three times with 1 \times PBS and stained with 4',6-diamidino-2-phenylindole (DAPI) in vectashield (0.2 g ml $^{-1}$, Vector Laboratories Inc.). Nuclear morphology was observed under fluorescence microscope.

4.8. Comet assay for checking DNA damage

Comet assay (also known as Single Cell Gel Electrophoresis Assay) is a facile method for measuring DNA strand breaks in eukaryotic cells. The term “comet” refers to the pattern of DNA migration through the

Table 5

Binding interactions of selected compounds with caspase-3 enzyme.

Sl. No.	Compound no.	Binding affinity (–Kcal/mol)	H-bond interaction sites	Hydrophobic interaction sites
1	3f	7.57	Arg 64, His 121, Gln 161, Arg 207	Ser 120, Gly 122, Cys 163, Gly 165, Thr 166, Trp 206, Tyr 204, Ser 205
2	3h	8.65	Ser 251	Thr 62, Ser 65, His 121, Cys 163, Tyr 204, Trp 206, Ser 209, Asp 253, Phe 256
3	3u	8.19	Asn 208, Ser 251	Tyr 204, Ser 205, Trp 206, Arg 207, Asn 208, Asp 253, Phe 256

electrophoresis gel, which often resembles a comet [57]. Frosted slide pre-coated with 200 μ L of 0.8% normal melting point of compound **3h** rose in PBS and left briefly to solidify. Cover slips were removed and MDA-MB-468 and MCF 7 cells (90 μ L) (3×10^5) were washed and resuspended in 100 μ L of low melting point agarose that was in turn pipetted onto the normal melting point agarose layer spread with cover slips and left briefly to solidify. Trypsin solution (50 μ L) was added onto the slide and left for 30 min at 37 °C. Slides were then immersed in ice-cold lysis solution (2.5 M NaCl, 100 mM EDTA, 10 mM Tris-HCl, pH-16, 1% Triton X-100, 10% DMSO) and incubated at 4 °C for 1 h. Then the slides were equilibrated in freshly prepared electrophoresis buffer (1 mM EDTA, 300 mM NaOH, pH-9.1) for 20 mins at 40 °C before performing electrophoresis. Electrophoresis was done for 20 mins at 25 V, 300 mA at room temperature. The slides were drained and washed three times with freshly prepared neutralizing buffer (0.4 M Tris-HCl, pH-7.5) for 20–30 mins. The slides were stained with 40 μ L of 20 μ g/mL of ethidium bromide and kept in dark until use. During the examination, the slides were washed with PBS three times and mounted with mounting medium and observed directly under fluorescence microscope. A total of about 50 cells per slide were analyzed for comet parameters using an image analysis system.

4.9. Western blot

Briefly, cell lysates were prepared from MDA-MB-468 and MCF7 cells with RIPA buffer method post treatment with various doses of compound **3h**. For immunoblotting, 20–35 μ g proteins were resolved on 8%–15% SDS-PAGE, transferred onto PVDF membrane (Millipore, USA), blocked with 5% BSA in 1 \times TBST, and probed with respective primary antibodies followed by corresponding secondary antibodies. Finally blots were developed into X-Ray films by ECL method.

4.10. Molecular docking study of three selective compounds

Molecular docking study was carried out through Autodock 4.2 software [59]. Before docking, all the structures (Compound **3f**, **3h** and **3u**) of the inhibitors were made in Chemdraw 10 and optimize their geometry using the default minimization algorithm. For docking study, the protein coordinates of Caspase-3 (PDB code: **1GFW**) [60] were prepared in Autodock. The molecules were located in the ligand area by using fit atom method [61]. The docking was made in Autodock by setting the grid size for the search as $60 \times 60 \times 60$ Å dispersed around the ligand binding site along with default grid spacing (0.375 Å) [58]. The molecules were allowed for flexible docking in the protein. 100 docking runs were performed for each molecule and the best docked poses were isolated by identifying their Gibbs free energies (ΔG) of the population. The interactions between protein and docked molecules were visualized in Autodock, Pymol and Discovery Studio Visualizer [61–63]. To validate docking experiments, all extracted ligands of all co-crystals were docked individually with their proteins to compare protein binding coordinates with the crystal forms and also identify the binding affinity. Furthermore, standard drug molecule was docked in the same protein coordinates of the co-crystal structure for comparison study with selected synthesized molecules.

4.11. Statistical analysis

All the experiments were conducted in triplicate. Data were represented as mean \pm SD. Data were subjected to One-way ANOVA analysis following students *t* test using GraphPad Prism 6.0 (USA). The data presented as the average of three experiments \pm SD. * = represents P value < 0.05, ** = represents P value < 0.01.

Acknowledgements

I.B. and K.P. thank CSIR, India for providing Junior and Senior

Research Fellowships respectively and U.D. thanks SERB, India for N-PDF fellowship. This work was supported by SERB, New Delhi, India (AKM) [Project No. EMR/2015/000282].

References

- [1] M.B. Sporn, D.L. Newton, *Fed. Proc.* 38 (1979) 2528–2534.
- [2] A.C. Begg, F.A. Stewart, C. Vens, *Nat. Rev. Cancer* 11 (2011) 239–253.
- [3] W.P. Steward, K. Brown, *Br. J. Cancer* 109 (2013) 1–7.
- [4] B.A. Chabner, T.G. Roberts, *Nat. Rev. Cancer* 5 (2005) 65–72.
- [5] N. Hail Jr., *Apoptosis* 10 (2005) 687–705.
- [6] A.L. Demain, P. Vaishnav, *Microbial. Biotechnol.* 4 (2011) 687–699.
- [7] J. Mann, *Nat. Rev. Cancer* 2 (2002) 143–148.
- [8] J. Jimeno, J.A. López-Martin, A. Ruiz-Casado, M.A. Izquierdo, P.J. Scheuer, K. Rinehart, *Anticancer Drugs* 15 (2004) 321–329.
- [9] B.S. El-Menshaw, W. Fayad, K. Mahmoud, S.M. El-Hallouty, M. El-Manawaty, M.H. Olofsson, S. Linder, *Indian J. Exp. Biol.* 48 (2010) 258–264.
- [10] D.J. Newman, G.M. Cragg, *Curr. Opin. Investig. Drugs* 10 (2009) 1280–1296.
- [11] B.C. Case, M.L. Hauck, R.L. Yeager, A.H. Simkins, M. deSerres, V.D. Schmith, J.E. Dillberger, R.L. Page, *Stem Cells* 18 (2000) 360–365.
- [12] L. Kma, *Asian Pac. J. Cancer Prev.* 14 (2013) 6197–6208.
- [13] R.J. Thoppil, A. Bishayee, *World J. Hepatol.* 3 (2011) 228–249.
- [14] T. Rabi, S. Gupta, *Front. Biosci.* 13 (2008) 3457–3469.
- [15] M.K. Chahar, N. Sharma, M.P. Dobhal, Y.C. Joshi, *Pharmacogn. Rev.* 5 (2011) 1–12.
- [16] T. Isah, *Pharmacogn. Rev.* 10 (2016) 90–99.
- [17] C. Spatafora, C. Tringali, *Anticancer Agents Med. Chem.* 12 (2012) 902–918.
- [18] X. Salvatella, E. Giral, *Chem. Soc. Rev.* 32 (2003) 365–372.
- [19] A.N. Jain, *Curr. Opin. Drug Discov. Develop.* 7 (2004) 396–403.
- [20] S.S. Young, N. Ge, *Curr. Opin. Drug Discov. Develop.* 7 (2004) 318–324.
- [21] J. Iqbal, B.A. Abbasi, T. Mahmood, S. Kanwal, B. Ali, S.A. Shah, A.T. Khalil, *Asian Pacific J. Trop. Biomed.* 7 (2017) 1129–1150.
- [22] I. Nwachukwu, A. Slusarenko, M. Gruhlke, *Nat. Prod. Commun.* 7 (2012) 395–400.
- [23] L.D. Lawson, B.G. Hughes, *Planta Med.* 58 (1992) 345–350.
- [24] L. Weiner, I. Shin, L.J.W. Shimon, T. Miron, M. Wilchek, D. Mirelman, F. Frolow, A. Rabinkov, *Protein Sci.* 18 (2009) 196–205.
- [25] J.T. Pinto, R.S. Rivlin, *J. Nutr.* 131 (3s) (2001) 1058s–1060s.
- [26] S. Oommen, R.J. Anto, G. Srinivas, D. Karunakaran, *Eur. J. Pharmacol.* 485 (2004) 97–103.
- [27] C. Jacob, *Nat. Prod. Rep.* 23 (2006) 851–863.
- [28] J. Borlinghaus, F. Albrecht, M.C. Gruhlke, I.D. Nwachukwu, A.J. Slusarenko, *Molecules* 19 (2014) 12591–12618.
- [29] T. Li, H.-Y. Shi, Y.-X. Hua, C. Gao, Q. Xia, G. Yang, B. Li, *Int. J. Clin. Expt. Pathol.* 8 (2015) 12525–12532.
- [30] S. Petropoulos, A. Fernandes, L. Barros, A. Ciric, M. Sokovic, I.C.F.R. Ferreira, *Food Chem.* 245 (2018) 7–12.
- [31] A. Rabinkov, T. Miron, L. Konstantinovskii, M. Wilchek, D. Mirelman, L. Weiner, *Biochim. Biophys. Acta.* 1379 (1998) 233–244.
- [32] F. Donato, N.F. Pavin, A.T. Rossito Goes, L.C. Souza, L.C. Soares, O.E.D. Rodrigues, C.R. Jesse, L. Savegnago, *Pharmaceut. Biol.* 53 (2015) 395–403.
- [33] S.J. Ahn, M. Koketsu, H. Ishihara, S.M. Lee, S.K. Ha, K.H. Lee, T.H. Kang, S.Y. Kima, *Chem. Pharm. Bull.* 54 (2006) 281–306.
- [34] M. Ninomiya, D.R. Garud, M. Koketsu, *Coord. Chem. Rev.* 255 (2011) 2968–2990.
- [35] O. Bouteira, G.J.L. Bernardes, M. Fernández-González, D.C. Anthony, B.G. Davis, *Angew. Chem. Int. Ed. Engl.* 124 (2012) 1461–1465.
- [36] M. Kogami, M. Koketsu, *Org. Biomol. Chem.* 13 (2015) 9405–9417.
- [37] I. Bhaumik, A.K. Misra, *Synopen* 1 (2017) 117–120.
- [38] A.K. Misra, G. Agnihotri, *Synth. Commun.* 34 (2004) 1079–1085.
- [39] T. Manna, A.K. Misra, *Synopen* 2 (2018) 229–233.
- [40] A. Sudalai, A. Khenkin, R. Neumann, *Org. Biomol. Chem.* 13 (2015) 4374–4394.
- [41] F. Silva, A. Baker, J. Stansall, W. Michalska, M.S. Yusubov, M. Graz, R. Saunders, G.J.S. Evans, T. Wirth, *Eur. J. Org. Chem.* (2018) 2134–2137.
- [42] S.W. Bass, S.A. Evans, *J. Org. Chem.* 45 (1980) 710–715.
- [43] F. Freeman, C.N. Angeletakis, *J. Am. Chem. Soc.* 105 (1983) 4039–4049.
- [44] K. Kondo, A. Negishi, *Tetrahedron* 27 (1971) 4821–4830.
- [45] P. Allen, J.W. Brook, *J. Org. Chem.* 27 (1962) 1019–1020.
- [46] K.L. Stensaa, A.S. Brownell, S. Ahuja, J.K. Harriss, S.R. Herman, *J. Sulfur Chem.* 29 (2008) 433–443.
- [47] T.J. Maricich, C.N. Angeletakis, *J. Org. Chem.* 49 (1984) 1931–1934.
- [48] W.E. Savage, A. Fava, *Chem. Commun.* 18 (1965) 417–418.
- [49] J. Kusterer, A. Vogt, M. Keusgen, *J. Agric. Food Chem.* 58 (2010) 520–526.
- [50] P.R. Twentyman, M. Luscombe, *Br. J. Cancer* 56 (1987) 279–285.
- [51] T. Mosmann, *J. Immunol. Methods* 65 (1983) 55–63.
- [52] P. Yuan, L. Di, X. Zhang, M. Yan, D. Wan, L. Li, Y. Zhang, J. Cai, H. Dai, Q. Zhu, R. Hong, *B. Xu, Medicine (Baltimore)* 94 (2015) e774, <https://doi.org/10.1097/MD.0000000000000774>.
- [53] E. Miller, *Methods Mol. Med.* 88 (2004) 191–202.
- [54] B. Halliwell, J. Gutteridge, *Free Radicals in Biology and Medicine*, Oxford University Press, Oxford, 2007.
- [55] E. Eruslanov, S. Kusmartsev, *Methods Mol. Biol.* 594 (2010) 57–72.
- [56] P.K. Parida, A. Sau, T. Ghosh, K. Jana, K. Biswas, S. Raha, A.K. Misra, *Bioorg. Med. Chem. Lett.* 24 (2014) 3865–3868.
- [57] A. Dhawan, M. Bajpayee, D. Parmar, *Cell. Biol. Toxicol.* 25 (2009) 5–32.
- [58] P.K. Parida, B. Mahata, A. Santra, S. Chakraborty, Z. Ghosh, S. Raha, A.K. Misra, K. Biswas, K. Jana, *Cell Death Dis.* 9 (2018) 448, <https://doi.org/10.1038/s41419-018-0000-0000>.

- 018-0476-2.
- [59] G.M. Morris, R. Huey, W. Lindstrom, M.F. Sanner, R.K. Belew, D.S. Goodsell, A.J. Olson, *J. Comput. Chem.* 30 (2009) 2785–2791.
- [60] D. Lee, S.A. Long, J.L. Adams, G. Chan, K.S. Vaidya, T.A. Francis, K. Kikly, J.D. Winkler, C.M. Sung, C. Debouck, S. Richardson, M.A. Levy, W.E. DeWolf Jr, P.M. Keller, T. Tomaszek, M.S. Head, M.D. Ryan, R.C. Haltiwanger, P.H. Liang, C.A. Janson, P.J. McDevitt, K. Johanson, N.O. Concha, W. Chan, S.S. Abdel-Meguid, A.M. Badger, M.W. Lark, D.P. Nadeau, L.J. Suva, M. Gowen, M.E. Nuttall, *J. Biol. Chem.* 275 (2000) 16007–16014.
- [61] U. Debnath, S. Verma, P. Singh, K. Rawat, S.K. Gupta, R.K. Tripathi, H.H. Siddiqui, S.B. Katti, Y.S. Prabhakar, *Chem. Biol. Drug Des.* 86 (2015) 1285–1291.
- [62] D. Seeliger, B.L. De Groot, *J. Comput. Aided Mol. Des.* 24 (2010) 417–422.
- [63] Discovery Studio Visualizer Software; 2012, Version 4.0. <http://www.accelrys.com>.